



Research Article

**ESTIMATION OF TRIANGULAR LABYRINTH SIDE WEIR DISCHARGE CAPACITY USING SCHMIDT APPROACH**

**Erdinc IKINCIÖGULLARI\*<sup>1</sup>, Muhammet Emin EMİROĞLU**

<sup>1</sup>Department of Civil Engineering, Bingöl University, BİNGÖL; ORCID: 0000-0003-2518-980X

<sup>2</sup>Civil Engineering Department, Firat University, ELAZIG; ORCID: 0000-0002-3603-0274

**Received: 05.01.2019 Revised: 14.02.2019 Accepted: 01.03.2019**

**ABSTRACT**

The labyrinth side weir is a new type of weir and a flow diversion apparatus. Labyrinth side weirs could overflow more discharge when compared to classical side weirs. The present study focused on the estimation of triangular labyrinth side weir discharge coefficients using the Schmidt approach. An accurate discharge coefficient should be estimated for the hydraulic design. In the study, various weir included angles, weir opening lengths, crest heights, flow depths, and Froude numbers were considered to estimate the flow characteristics of the labyrinth side weir. 2623 experimental runs were conducted for the triangular side weir. Furthermore, to estimate the discharge capacity, the nape height was determined at two (as proposed by Schmidt) and three points in the present study. The compatibility of the average nape height that was proposed by Schmidt was examined with supplementary laboratory tests. Furthermore, the findings were compared to the literature and confirmed the usability of the Schmidt approach. This study demonstrated that the Schmidt approach was consistent with the tendencies in the literature in determining the discharge capacity and produced a useful graphical presentation for hydraulic designers. The Schmidt approach was quite reliable in calculating triangular labyrinth side weir discharge capacity.

**Keywords:** Side weirs, discharge coefficient, schmidt approach, discharge capacity, de marchi approach, triangular labyrinth side weirs.

**1. INTRODUCTION**

Side weirs are utilized to decrease water discharge or to reduce the flow level. It is situated parallel to the canal axle or with an angle to the canal wall to canalize flow from the canal. Lateral overflow structures are utilized in the following application areas: Urban drainage systems (combined sewer systems), irrigation engineering (open distribution canals), lateral intake (power stations), river bifurcations (flow diversions), river restorations (ecological flooding), side overflow spillway at dam reservoirs, and flood control management (reducing the peak flow using retention basins or flood plains). In narrow canyons or where the width of the control structure site is limited, the spillway crest is situated parallel to the canal. This is named a side canal spillway. Labyrinth side weirs are also utilized as side canal spillways. Furthermore, canal overflow with runoff could be removed using side weirs. The side weir could balance water loss that emerges due to below-efficient irrigation operations.

\* Corresponding Author: e-mail: erdincikinciogullari@gmail.com, tel: (426) 216 00 32 / 1966

Labyrinth weirs are composed of a row of straight weirs folded in a zigzag fashion providing a longer weir crest length than a straight weir for a given weir site. The labyrinth spillway is an efficient and economical solution that increases the weir crest length without the associated increase in structure breadth, thus increasing the discharge. The labyrinth spillway use in reservoirs is especially adequate for sites with limited weir breadth and upstream water surface and where larger discharge capacities are required. A labyrinth weir has advantages when compared to conventional weirs, and weirs with ogee-crest ([1], [2], and [3]). The labyrinth weir could be used as a side weir ([4]).

Side weirs possess different types of cross-sections (for example; trapezoidal, triangular, rectangular and circular). Conventional side weirs could be located parallel to the canal axle or angled to the canal wall. The plan orientation of labyrinth side weirs could be triangular, trapezoidal, and elliptic. However, trapezoidal labyrinth side weirs are the best in terms of construction and hydraulic performance criteria ([4] and [5]).

Every type of weir has different hydraulic properties. Therefore, the flow characteristic of a weir type is important. This requires examination of each weir separately, especially the labyrinth side weirs. There are several publications on classical side weirs in the literature. Labyrinth side weirs with a triangular or trapezoidal shape were scrutinized here. The labyrinth side weir is a modern type of weir, and it was initially introduced by Emiroglu et al. [5].

The spatially varied flow (SVF) is characterized by a non-uniform discharge resulting from the addition or reduction of water flow along the open canal. The discharge decreases with the weir opening length. The lateral flow hydraulics is complex. The effect of secondary flow is very important for the side weirs. The water surface behavior was discussed to explain the secondary flow effect that occurs because of lateral flow near the downstream end of the side weir.

Several studies have been carried out side weir discharge coefficients. In the literature, there are several experimental and theoretical studies. Although De Marchi [6] introduced the first approach to side weirs, there is still no clear information about the variations in discharge coefficients.

Bonakdari et al. [7] researched a modified triangular side weir. They estimated the discharge coefficient of that triangular side weir using the Adaptive Neuro-Fuzzy Inference System (ANFIS). They modeled the discharge coefficient using dimensionless input variables with ANFIS, artificial neural network, support vector machine, and multi nonlinear regression methods. They reported that ANFIS could correctly estimate the discharge capacity for modified triangular side weirs. Seyedian et al. [8] also studied side weir discharge coefficient using ANFIS.

Aydin [9] proposed a new semi-analytical approach to solve discharge capacity of rectangular side weirs because of the De Marchi approach is difficult in practice. Moreover, Aydin and Kayisli [10] predicted discharge capacity over to cycle labyrinth side weir using ANFIS. Aydin [11] modeled CFD simulation of triangular labyrinth side weir and compared with experimental results and good agreements obtained.

The hydraulics of the side weir was a significant topic in the literature. De Marchi method was frequently applied to determine the discharge capacity. Although Schmidt [12] introduced a significant approach for discharge capacity, there are only a few studies conducted with Schmidt's method in the literature.

De Marchi hypothesis was used frequently in the literature. However, there are other approaches besides the De Marchi method to determine the discharge capacity of side weirs such as Schmidt, Stopsack, and Dominguez methods. As far as we know, the Schmidt method has not been used to guess the triangular labyrinth side weir discharge capacity. De Marchi hypothesis was used frequently in the literature. However, there are other approaches besides the De Marchi method to guess the discharge capacity of side weirs including Schmidt, Stopsack, and Dominguez methods. As far as we know, the Schmidt method was not used to determine the triangular labyrinth side weir discharge capacity. The goal of the current study is to examine the hydraulic properties of triangular labyrinth side weirs using the Schmidt approach. Furthermore,

the obtained findings were compared to other studies in the literature to test the dependability of the Schmidt method in estimating the discharge capacity of the labyrinth side weirs. The present study further aimed to provide useful findings and graphs for hydraulic designers.

### 3. THEORETICAL BACKGROUND

#### 3.1. De Marchi Approach

De Marchi hypothesis was used frequently in the literature. However, there are other approaches besides the De Marchi method to determine the discharge capacity of side weirs including Schmidt, Stopsack, and Domínguez methods. As far as we know, the Schmidt method was not used to determine the triangular labyrinth side weir discharge capacity.

Spatially varied flow is characterized by a non-uniform discharge resulting from the addition or reduction of water on the flow direction. The flow over a side weir is a typical case of spatially varied flow with a decreasing discharge. Theoretically, De Marchi [6] presented a method to resolve water surface differential equation for side weirs. De Marchi was the first scientist, who provided an analytical solution for estimating the water surface profile along a rectangular side weir with rectangular cross-section in an open canal and this solution made a significant contribution to this problem. This solution is based on the constant weir coefficient, constant velocity distribution coefficient and constant specific energy along the side weir. For side weirs in rectangular canals, the abovementioned assumptions and further constructed hypotheses allowed De Marchi to obtain the analytical integration of the spatially varying flow equation (with decreasing discharge). De Marchi demonstrated that the water flow profile is curved, rising in subcritical flow regime and decreasing in supercritical flow regime. Additionally, De Marchi approach was used in several side weir shapes (triangular, trapezoidal and circular) and types (sharp-crested weir, broad crested weir and labyrinth weir) in the literature ([13]; [14]; [7]). Paris et al. [15] and Michelazzo et al. [16] proved the feasibility of the De Marchi approach for lateral flow in the case of movable beds.

$$C_d = \frac{3}{2} \frac{B}{L} (\Phi_2 - \Phi_1) \tag{1}$$

In which,  $C_d$  is the discharge coefficient,  $B$  is the channel width and  $L$  is the side weir opening. Based on Eq. (1), De Marchi investigated a correlation between  $C_d$ , canal width, side weir length, and  $\Phi$ . Here,  $\Phi_1$  and  $\Phi_2$  reflect immediate side weir upstream and downstream, respectively.  $C_d$  has to be found experimentally. Eq. (2) could be utilized to calculate  $\Phi_1$  and Eq. (3) could be used to determine the flow rate.

$$\Phi_1 = \frac{2E_1 - 3p}{E_1 - p} \sqrt{\frac{E_1 - y_1}{y_1 - p}} - 3 \sin^{-1} \left( \sqrt{\frac{E_1 - y_1}{E_1 - p}} \right) \tag{2}$$

$$Q_w = \frac{2}{3} C_d \sqrt{2g} L (y_1 - p)^{3/2} \tag{3}$$

in which  $Q_w$  is the side weir discharge ( $m^3/s$ ),  $E$  is the specific energy,  $y$  is the main flow depth,  $L$  is the opening length of the side weir,  $B$  is the breadth of the canal,  $p$  is the crest height and  $g$  is the acceleration of gravity.

#### 3.2. Schmidt Approach

Schmidt [12] determined the discharge capacity of the side weir under subcritical flow regime. Specific energy variation is given in Fig. 1 (a). Based on Fig. 1 (a), the energy equation is calculated as shown in Eq. (4);

$$S_0 L + p + h_1 + \alpha_1 \frac{V_1^2}{2g} = h_3 + p + \alpha_2 \frac{V_2^2}{2g} + \Delta h_s \tag{4}$$

$$h_1 = h_3 + \alpha_2 \frac{V_2^2}{2g} - S_0 L - \alpha_1 \frac{V_1^2}{2g} + \Delta h_s \quad (5)$$

where,  $S_0$  is the slope of the canal,  $h_1$  is the nappe height at upstream of the side weir,  $h_3$  is the nappe height at side weir downstream,  $V$  is the mean velocity,  $\alpha_1$  and  $\alpha_2$  are the energy correction coefficients and  $\Delta h_s$  is the friction loss. The  $\Delta h_s$  can be solved with the Manning-Strickler formula.

As shown in Fig. 1, the labyrinth side weir has no straight crest in the canal plan. The nappe height at upstream end of the side weir is reduced with an increasing crest length for a specified flow. Hence, side weirs are advantageous when the weir opening length is limited or more water is required. The type of side weir, canal cross section, and angle of the side weir changes the amount of overflow.

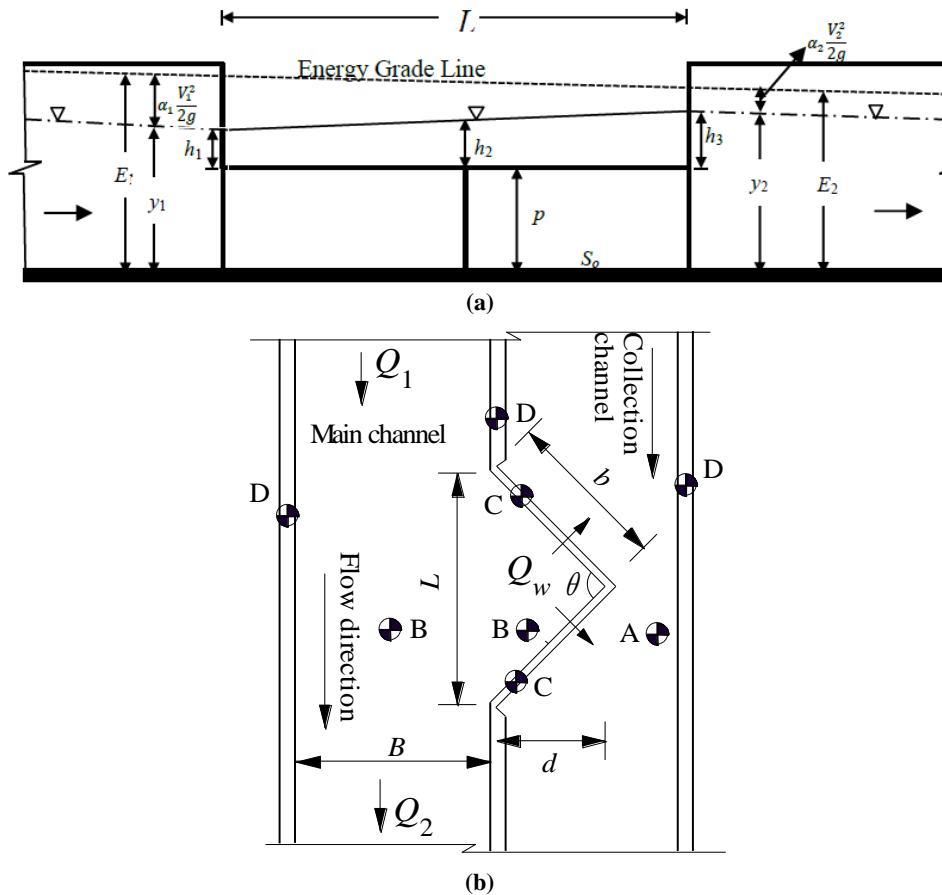


**Figure 1.** Definition of labyrinth side weirs (a) Longitudinal section;  
 (b) Plan (El. A=0.73 m, El. B=0.93 m, El. C=1.05 m, 1.09 and 1.13 m, El. D=1.43 m)

In Fig. 1, b is the half-crest length of the labyrinth side weir,  $\theta$  is the angle of the triangular side weir and  $h_2$  is the nappe height at center of the side weir. Term  $Q_1$  is the discharge at side weir

upstream and  $Q_2$  is the discharge at side weir downstream. Thus,  $Q_w=Q_1-Q_2$  could be used to calculate the flow rate over the side weir.

Energy correction coefficients can be accepted as  $\alpha_1=\alpha_2=1.1$  with using the trial and error method. Experimentally estimated  $\xi$  was used to right the energy correction coefficients. Eq. (6) was formulated for  $\Delta h_s = S_F L \cong S_0 L$ ,

$$h_1 = h_2 - \xi \left[ 1.1 \frac{V_1^2}{2g} - 1.1 \frac{V_2^2}{2g} \right] \tag{6}$$

where  $\xi$  is the correction coefficient according to the Schmidt method.

The Poleni equation was utilized to solve the discharge coefficient in the Schmidt method.

$$C_d = \frac{3}{2} \frac{Q_w}{\sqrt{2g} L h_a^{3/2}} \tag{7}$$

$$Q_w = \frac{2}{3} C_d \sqrt{2g} L h_a^{3/2} \tag{8}$$

$$h_a = \frac{1}{2} (h_1 + h_2) \tag{9}$$

$$*h_a = \frac{1}{3} (h_1 + h_2 + h_3) \tag{10}$$

$$*C_d = \frac{3}{2} \frac{Q_w}{\sqrt{2g} L *h_a^{3/2}} \tag{11}$$

where  $*C_d$  is the discharge coefficient based on three points,  $h_a$  is average nappe height based on two points and  $*h_a$  is average nappe height based on three points. Here, to examine the credibility of the results obtained with two points (according to Schmidt approach), the nappe heights were calculated based on three points using Eq. (10).

According to Schmidt's method, Eq. (12) could be used instead of Eq. (6) where the friction loss was considered in the formula or where the crest length is much larger [17].

$$\xi = \frac{h_2 - h_1}{1.1 \frac{V_1^2}{2g} - 1.1 \frac{V_2^2}{2g} - \Delta h_s} \tag{12}$$

This approach is valid for the case where there are subcritical flow regime inflow and subcritical flow regime outflow. The use of the Schmidt approach is not adequate in situations where a hydraulic jump takes place along the side weir opening length.

In the Schmidt approach, mean nappe load can be used as given in Eq. (9 and 10). If the weir opening length is too long, the nappe load for Schmidt approach can be measured at a higher number of points, thus the mean nappe load can be determined more accurately. In De Marchi approach, only the nappe loads at the upstream and downstream ends of the side weir are used in Eq. (1 and 3)

#### 4. SENSITIVITY ANALYSIS

The sensitivity analysis was used to evaluate the relative significance of each parameter vis a vis any other parameter. The predicted value obtained with equation was compared with the value measured in the experiment. The accuracy of any measured value could be determined using certain methods such as the root mean square errors (RMSE), correlation coefficient (R) and mean absolute errors (MAE).

The RMSE is a frequently used measure between the measured value and the predicted value. The MAE is utilized to measure how close predictions were to eventual outcomes. The RMSE and MAE are described as:

$$RMSE = \sqrt{\frac{1}{N} \sum_{i=1}^N (Q_{i_{measured}} - Q_{i_{predicted}})^2} \tag{13}$$

$$MAE = \frac{1}{N} \sum_{i=1}^N |Q_{i_{measured}} - Q_{i_{predicted}}| \tag{14}$$

where N is the data set number, i is the number of series.

The correlation coefficient (R) is the statistical correlation between two or more values in fundamental statistics.

$$R = \frac{\sum_{i=1}^N (Q_{i\text{measured}} - \overline{Q_{i\text{measured}}})(Q_{i\text{predicted}} - \overline{Q_{i\text{predicted}}})}{\sqrt{\sum_{i=1}^N (Q_{i\text{measured}} - \overline{Q_{i\text{measured}}})^2 \sum_{i=1}^N (Q_{i\text{predicted}} - \overline{Q_{i\text{predicted}}})^2}} \quad (15)$$

in which  $\overline{Q_{i\text{predicted}}}$  and  $\overline{Q_{i\text{measured}}}$  are the mean predicted discharge and the mean measured discharge, respectively.

The Nash- Sutcliffe (DC) efficiency coefficient was utilized to appraise the estimation strength of hydrological models.

$$DC = 1 - \frac{\sum_{i=1}^N (Q_{i\text{measured}} - Q_{i\text{predicted}})^2}{\sum_{i=1}^N (Q_{i\text{measured}} - \overline{Q_{i\text{measured}}})^2} \quad (16)$$

### 5. EXPERIMENTAL SETUP

2623 experimental runs were conducted with the triangular side weir. Experimental data reported by Emiroglu et al. [4] and Emiroglu and Kaya [18] were used for this purpose. The experimental setup is presented in Fig. 4. The width of the main and the collection canal breadth was 0.50 m. The main canal depth was 0.50 m and the collecting canal depth was 0.70 m. Three different weir lengths (0.25, 0.50, and 0.75 m) and weir heights (0.12, 0.16, and 0.20 m) were set up in the present study. The canal slope was 0.001.

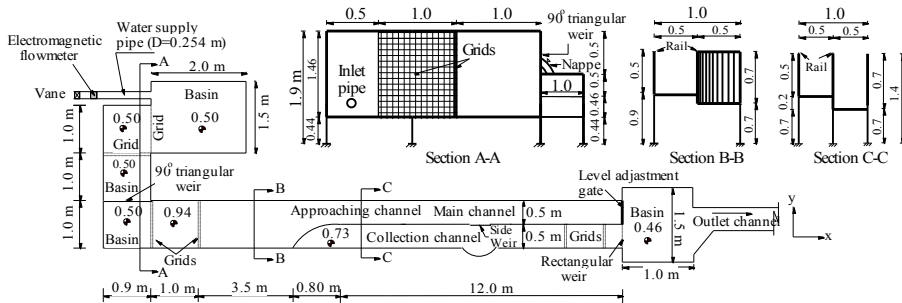


Figure 4. Experimental setup

The side weir was placed at an appropriate distance from the flow inlet to ensure fully developed flow conditions. Commonly, the hydrodynamic entry length needs to be distant from the pipe entrance where the wall shear stress reaches within 2 percent of the fully developed value. In the case of laminar flow, the hydrodynamic entry length is 0.05Re. In the case of turbulent flow, the hydrodynamic entry length is 10D where Re = Reynolds number and D = pipe diameter. The experiments should be conducted within the fully developed flow region. Therefore, the experiments were implemented at the “fully developed flow” zone. The hydrodynamic entry length for open canal flows is given by Kirkgoz and Ardicioglu [19] as below.

$$\frac{L_d}{y} = 76 - 0.0001 \frac{Re}{F} \quad (17)$$

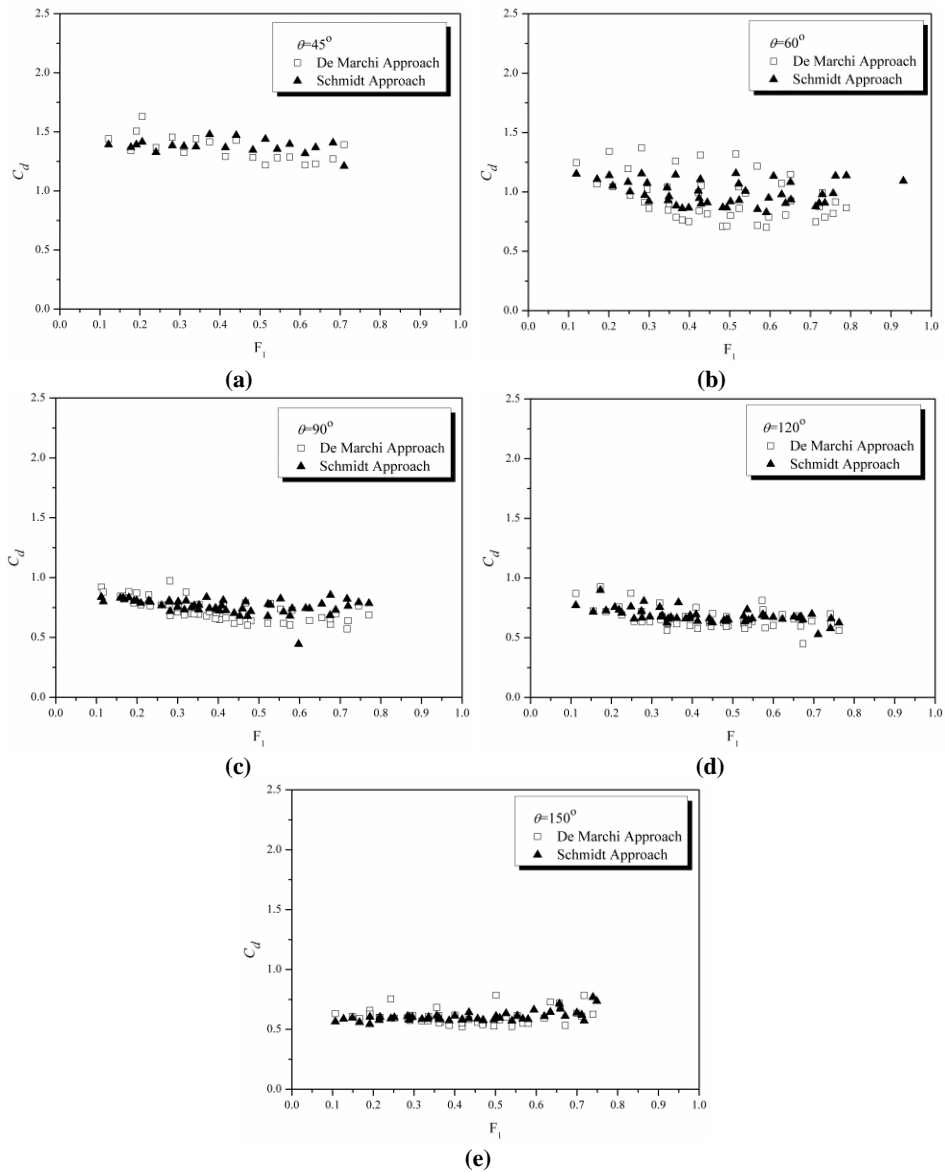
where  $L_d$  is the length of flow developing zone. In this study, the side weirs were placed 3 m after entering the experimental canal.

The flow rate sensitivity was measured as  $\pm 0.01$  l/s using a Siemens brand electromagnetic flow-meter. The water depths were measured as  $\pm 0.01$  mm with a Mitutoyo brand digital point gauge. Flow velocity sensitivity was measured as  $\pm 1$  mm/s by Acoustic Doppler high sensitivity velocity-meter. The minimum nappe height was 0.03 m. The discharge values were determined between 1.156 and 77.737 l/s. The Froude number varied between 0.069 and 0.998. Five different weir angles ( $45^\circ$ ,  $60^\circ$ ,  $90^\circ$ ,  $120^\circ$ , and  $150^\circ$ ) were utilized for the triangular side weirs. The discharge coefficient was estimated using the De Marchi and Schmidt approaches. Equation (1) and Eq. (7) were used to determine discharge capacity according to De Marchi and Schmidt methods, respectively. Furthermore, to test the compatibility of the mean nappe height as taken into consideration by Schmidt, Eq. (11) was considered to determine the discharge coefficient ( $*C_d$ ) with the Schmidt method. During the experiments, a hydraulic jump was not observed. Hence, there was no hesitation in using the Schmidt method for solving of discharge coefficient of the side weirs. These experiments were conducted under subcritical flow regime. The relative specific energy was fairly small at 4% for this study. Thus, it was also possible to use the De Marci approach safely.

## 6. RESULTS AND DISCUSSION

Parameters of  $F_1$ ,  $p$ ,  $L/B$ ,  $[(y_1-p)/p]$ , and  $\theta$  were considered for the triangular side weir. De Marchi and Schmidt methods were compared to test the credibility of the Schmidt method in estimating the triangular labyrinth side weir discharge coefficient. Eq. (1) and Eq. (7) were utilized to solve the discharge coefficient for De Marchi and Schmidt methods, respectively.

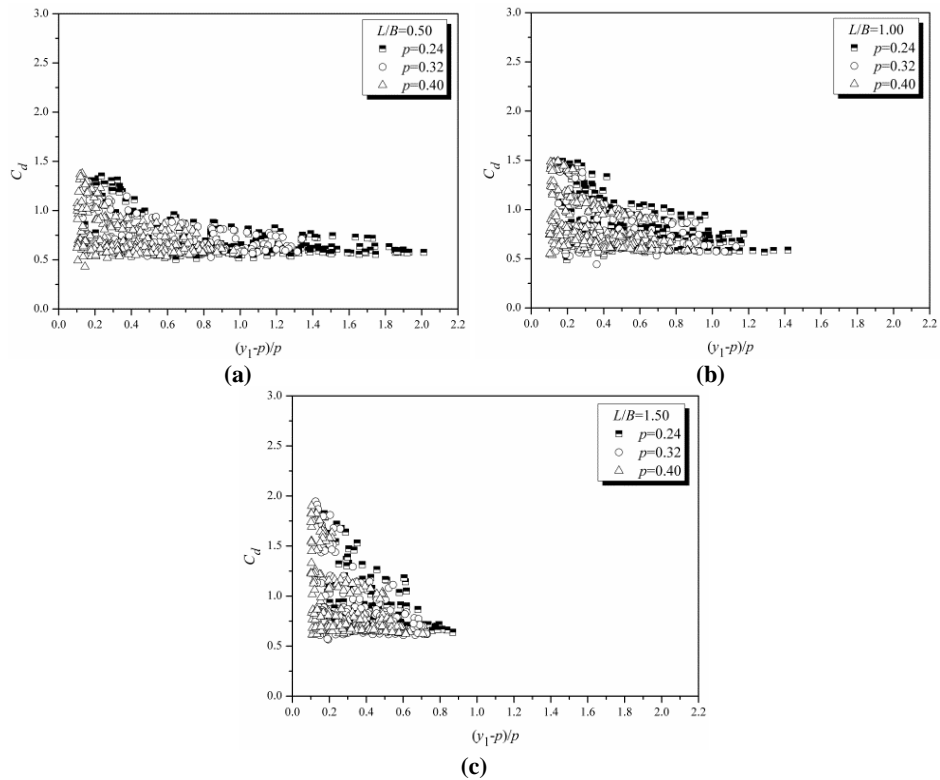
Figure (5) was plotted with the variations of  $C_d$  and  $F_1$  with constant  $L/B=1.00$ ,  $p=0.16$  cm, and in various weir angles ( $\theta$ ). Compatibility of the Schmidt and De Marchi methods were observed as presented in Fig. (5).  $C_d$  had a decreasing tendency with increasing  $F_1$  values for two approaches except  $\theta = 150^\circ$ . According to Fig. 5 (e),  $C_d$  exhibited an increasing tendency for  $\theta = 150^\circ$ .



**Figure 5. (a-e).** The dispersion of the methods for  $C_d$  vs.  $F_1$  were: (a) for  $\theta = 45^\circ$ ; (b) for  $\theta = 60^\circ$ ; (c) for  $\theta = 90^\circ$ ; (d) for  $\theta = 120^\circ$ ; and (e) for  $\theta = 150^\circ$

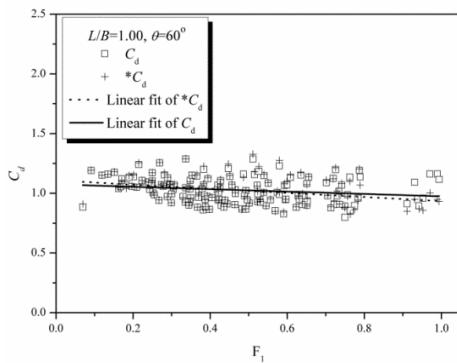
De Marchi results are more diffused than those of the Schmidt method. Therefore, a higher correlation coefficient was obtained using the Schmidt method. Furthermore, the formalization of the Schmidt method is easier when compared to the De Marchi method. For this reason, it was determined that the Schmidt approach was trustier for estimating the discharge coefficient. In addition,  $C_d$  decreased with the increase in weir angle.  $C_d$  was about 1.5 for the smallest weir angle (for  $\theta=45^\circ$ ). However, it decreased to about 0.5 for the largest weir angle (for  $\theta=150^\circ$ ).

Figure 6 demonstrates the variation of dimensionless nappe height  $[(y_1-p)/p]$  and  $C_d$ , which were estimated using the Schmidt approach. According to Fig. 4,  $C_d$  decreased with an increase in  $[(y_1-p)/p]$ . Emiroglu et al. [5] proved that  $C_d$  decreases when nappe height increases in labyrinth side weirs. However, the decrease in the rectangular side weir was significantly lower when compared to the labyrinth side weir. The decreasing tendency of  $C_d$  in higher  $L/B$  ratios was greater than that of the small  $L/B$  ratios. As shown in Fig. 4(a-c) that as  $L/B$  ratio raises  $C_d$  values also rise. The discharge coefficient increased with the raising dimensionless weir length  $L/B$  due to the secondary flow effect. In other words, because of the increase at the intensity of secondary flow created by the lateral flow, higher  $C_d$  values were obtained at high  $L/B$  ratios. El-Khashab [20] also talked about that the secondary flow condition is dominant because of lateral flow when a side-weir is relatively long (i.e.,  $L/B > 1$ ).



**Figure 6 (a-c).** Variation of  $[(y_1-p)/p]$  with  $C_d$  as estimated with the Schmidt method

Based on the Schmidt approach, the average nappe height was calculated with Eq. (9). The average nappe height was calculated using the two nappe heights that were measured at the upstream and downstream ends of side weir. In the present study, the average nappe height was calculated with Eq. (10) to test the compatibility of the two nappe heights. As seen in Eq. (10), three points on the upstream, side weir center and downstream ends of side weir were used in the computation of the average nappe height.  $*C_d$  was calculated with Eq. (11). Then,  $C_d$  and  $*C_d$  were compared as shown in Fig. (7). The tendencies in  $C_d$  and  $*C_d$ , based on Froude number were similar. Thus, the estimation of discharge capacity with two points was enough for the right results.



**Figure 7.** Comparison of  $C_d$  and  $*C_d$  for triangular side weirs

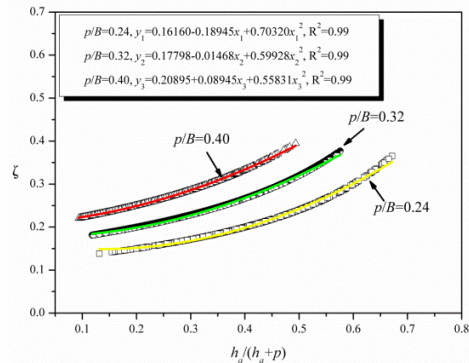


**Figure 8.** Variation of  $(\xi)$  with  $[h_a/(h_a+p)]$

The variation of correction coefficient ( $\xi$ ) was plotted with dimensionless nappe height  $[h_a/(h_a+p)]$  for constant crest height ( $p$ ) as shown in Fig. (8). There was an increasing tendency on  $\xi$  value for every crest high. Furthermore, as the crest height increased, the  $\xi$  value increased as well. As mentioned above,  $\xi$  was determined experimentally. In this study, to estimate  $\xi$  value, three different equations were constructed using the curve fitting method ( $R^2=0.99$ ). A hydraulics designer could easily utilize Fig. (8) to calculate the value of  $\xi$ .

Borghei et al. [14] investigated triangular labyrinth side weirs having one and two cycles and gave the following equation:

$$C_d = \frac{-0.269 \left( \frac{L}{B \sin(\frac{\theta}{2})} \right)^{-1.188} + \left( \frac{p}{y_1 - p} \right)^{0.18}}{1 + 0.649 \left( \frac{1}{\sin(\frac{\theta}{2})} \right)^{-0.505} + 0.056 \left( \frac{F_1}{\sin(\frac{\theta}{2})} \right)^{-1.275}} \quad (18)$$

where,  $\theta$  is the triangular labyrinth side weir inclusion angle.

As a result of experimental studies, Emiroglu et al. [5] proposed Eq. (19) for triangular labyrinth side weirs with one cycle.

$$C_d = 0.4 + \left[ \begin{array}{l} -2.62 + 0.634 \left( \frac{L}{B} \right)^{0.254} + 3.214 \left( \frac{L}{L_{ef}} \right)^{-0.122} \\ -0.684 \left( \frac{p}{y_1} \right)^{-0.4} + 0.122 \left( \sin \left( \frac{\theta}{4} \right) \right)^{1.982} + 0.22 F_1^{2.458} \end{array} \right]^{3.857} \quad (19)$$

To test the credibility of the Schmidt method, the  $Q_w/Q_1$  obtained with the Schmidt approach was compared with the discharge obtained with Borghei et al. [14] and Emiroglu et al. [5] equations for triangular labyrinth side weir. Similar tendencies were observed with these three equations as shown in Fig. 9.

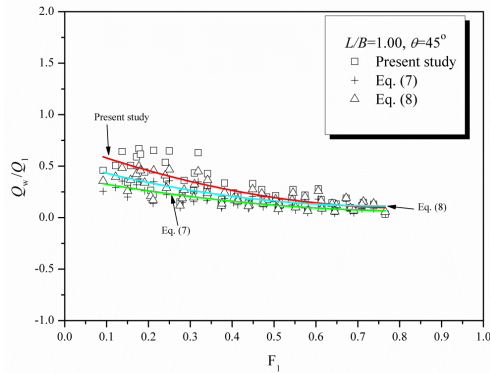


**Figure 9.** Compatibility of  $Q_w/Q_1$  for Schmidt Approach (present study), Eq. 18 and Eq. 19

Sensitivity analysis was used to calculate the error ratio between the discharge measured in the experiments and the discharge predicted with De Marchi and Schmidt approaches. In this study, the root mean square error (RMSE), mean absolute error (MAE), Nash and Sutcliffe (DC), and correlation coefficient (R) were examined for De Marchi and Schmidt approaches.

As shown in Table 1, the sensitivity analysis was investigated for total experimental results and it was found that RMSE was 4.88, MAE was 3.03 and DC was 0.91 with the Schmidt approach. However, it was found that RMSE was 7.36, MAE was 4.33 and DC was 0.81 with the De Marchi approach. The determination coefficients ( $R^2$ ) for Schmidt and De Marchi approaches were 0.96 and 0.86, respectively. It was concluded that the Schmidt method was more dependable for estimating the discharge coefficient based on the findings.

**Table 1.** The results of sensitivity analysis for Schmidt and De Marchi approaches

	Schmidt Approach	De Marchi Approach
RMSE	4.88	7.36
MAE	3.03	4.33
DC	0.91	0.81
$R^2$	0.96	0.86

Many researchers studied the classical side weir design experimentally ([21]; [22]; [23]; [24]; [25]; [5]; [26]). El-Khashab and Smith [21] introduced a general equation for a rectangular canal cross section and Eq. (20) could be utilized to assess the water surface profile over a side weir.

$$\frac{dy}{dx} = \frac{S_0 - S_E - \left(\frac{\alpha Q}{gA^2}\right) \frac{dQ}{dx}}{1 - \left(\frac{\alpha Q^2 B}{gA^3}\right)} \tag{20}$$

where  $x$  is the direction of flow,  $S_E$  is the energy grade line slope, and  $A$  is the cross-section area.

Hager [22] provided Eq. (21) to solve the conventional side weir discharge capacity. Borghei et al. [14] proposed Eq. (22) based on experimental results for sharp-crested rectangular side weir in subcritical flow regime.

$$C_d = 0.485 \left(\frac{2+F_1^2}{2+3F_1^2}\right)^{0.5} \tag{21}$$

$$C_d = 0.7 - 0.48F_1 - 0.3\left(\frac{p}{y_1}\right) + 0.06\left(\frac{L}{B}\right) \tag{22}$$

Several researchers carried out experimental studies on labyrinth side weirs ([1]; [2]; [4]; [5]; [14]; [18]; [26]). Ura et al. [27] studied oblique side weirs instead of labyrinth side weirs and submitted Eq. (23);

$$C_d = 0.611 \left[ \cos(\beta) \cdot \left( \frac{3F_1^2}{2+F_1^2} \right)^{0.5} + \sin(\beta) \cdot \left( 1 - \frac{3F_1^2}{2+F_1^2} \right)^{0.5} \right] \cdot \sin(\beta) \tag{23}$$

in which  $C_d$  is the discharge coefficient,  $F_1$  is the Froude number, and  $\beta$  is the influential oblique angle.

Emiroglu et al. [28] studied labyrinth side weirs having one and two cycles for subcritical flow regime. They used experimental data and came up with Eqs. (24, 25) via the De Marchi approach. Eq. (24) and Eq. (25) were proposed for one cycle side weirs and two-cycle trapezoidal labyrinth side weirs, respectively.

$$C_d = \left[ -10.054 \left( F_1 \frac{L_{ef}}{L} \right)^{0.039} - 0.001 F_1 \left( \frac{L}{B} \right)^{-6.79} - 0.438 \left( \frac{L_{ef}}{L} \right)^{-0.284} \right]^{-3.64} + 0.52 F_1 \left( \frac{y_1-p}{p} \right)^{-0.114} + 11.178 \left( F_1 \frac{y_1-p}{p \cdot \sin \alpha'} \right)^{0.013} \tag{24}$$

$$C_d = \left[ -0.001 (F_1)^{-1.78} + 0.10 \left( \frac{L}{B} \right)^{0.22} - 2.036 \left( \frac{y_1-p}{p} \right)^{0.03} \right]^{5.77} + 2.82 \left( \frac{L_{ef}}{L \cdot \sin \alpha'} \right)^{0.02} \tag{25}$$

in which,  $L_{ef}$  is the overflow length of the weir, and  $\alpha'$  is the sidewall angle.

Equations 18, 19 21, 22, and 23 are compared based on the Froude number, as illustrated in Fig. 10. As seen in Fig. 10, the decreasing tendency in  $C_d$  values with increasing Froude number in labyrinth side weirs was very small when compared to the classical side weirs. This can be also observed in Fig. 5(a-e). The decreasing tendency in  $C_d$  values with increasing Froude number in classical rectangular side weirs was higher when compared to other side weirs. This is due to the following factors: (1) The labyrinth weirs have more crest length. (2) Even in the case of high Froude numbers, the orientation of the streamlines towards the labyrinth side weir causes the discharge capacity to increase. (3) The nappe load in labyrinth side weirs is lower than the conventional side weir for the same outflow weir discharge. (4) Secondary flow intensity in the labyrinth side weir is more severe than the classical side weir. Therefore, the discharge capacity of labyrinth side weirs is 1.5 to 4.5 times higher than conventional side weirs for the same weir opening length.

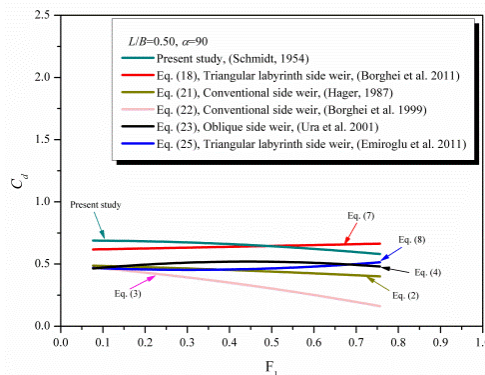


**Figure 10.** Comparison of variation  $C_d$  versus Froude number for labyrinth side weir and classical side weir

## 7. CONCLUSION

Until now, the De Marchi method was frequently utilized to calculate the discharge capacity of side weirs. In the current study, the discharge coefficient of the triangular labyrinth side weir was estimated utilizing the Schmidt method. The discharge coefficient ( $C_d$ ) varied inversely with Froude number ( $F_1$ ) and the dimensionless nappe height  $[(y_1-p)/p]$ . The results obtained with the Schmidt approach was then compared to those obtained with De Marchi methods and those found in the literature. Furthermore, the sensitivity analysis was examined for Schmidt and De Marchi approaches. RMSE are 4.88 and 7.36; MAE are 3.03 and 4.33; DC are 0.91 and 0.81;  $R^2$  are 0.96 and 0.86 for Schmidt and De Marchi Approaches, respectively. The results indicated that the variation of discharge capacity with the Schmidt approach exhibited similar tendencies when compared to the findings in the literature. Furthermore, the nappe height in two points, as proposed by Schmidt, was enough to calculate the average nappe height and it could be utilized to obtain accurate findings. We concluded that the Schmidt method is a dependable approach to determine the discharge capacity, hence, hydraulic designers can utilize the Schmidt approach with confidence for this purpose.

## Acknowledgments

The authors would like to thank Dr. Nihat Kaya (Firat University, Turkey) for their contributions.

## 8. Notation

A	: canal cross-section area ( $m^2$ )
B	: canal breadth (m)
b	: half-crest length of the labyrinth side weir (m)
$C_d$	: discharge coefficient (-)
E	: specific energy (m)
$F_1$	: Froude number (-)
g	: acceleration of gravity ( $m/s^2$ )
$h_a$	: average nappe height (m)
* $h_a$	: average nappe height calculated for Eq. (18) (m)
$h_1$	: nappe height at side weir upstream end (m)
$h_2$	: nappe height at side weir downstream end (m)
$h_3$	: nappe height at side weir center (m)
i	: number of series (-)
$S_E$	: energy slope (-)
$S_0$	: slope of canal(-)
L	: side weir opening length (m)
$L_d$	: flow developing length Region (m)
N	: number of data set (-)
p	: weir crest (m)
Re	: Reynolds number (-)
$Q_w$	: flow rate over side weir ( $m^3/s$ )
$Q_1$	: flow rate in the main canal upstream ( $m^3/s$ )
$Q_2$	: flow rate in the main canal downstream ( $m^3/s$ )
x	: distance along the side weir measured from upstream to end of side weir (m)
$V_1$	: mean velocity at upstream of side weir (m/s)
$V_2$	: mean velocity at downstream of side weir (m/s)
$y_1$	: flow depth at upstream end of side weir (m)

- $y_2$  : flow depth at downstream end of side weir (m)  
 $\Phi_1, \Phi_2$  : varied flow function (-)  
 $\Delta h_s$  : friction loss (m)  
 $\alpha'$  : trapezoidal side weir sidewall angle (-)  
 $\alpha_1, \alpha_2$  : kinetic energy correction coefficients (-)  
 $\theta$  : included angle of triangular labyrinth side weir (-)  
 $\xi$  : correction coefficient (-)  
 $\beta$  : influential oblique angle of oblique side weirs (-)

## REFERENCES

- [1] Kabiri-Samani A, Borghei SM and Esmaili H. Hydraulic performance of labyrinth side weirs using vanes or piles. *Proceedings of the Institution of Civil Engineers - Water Management*, 164(5): 229-241, (2011).
- [2] Kabiri-Samani A, Javaheri A and Borghei SM. Discharge coefficient of a rectangular labyrinth weir. *Proceedings of the Institution of Civil Engineers - Water Management* 166(8): 443-451, (2013).
- [3] Khode BV, Tembhurkar, AR, Porey PD and Ingle RN. Experimental studies on flow over labyrinth weir. *Journal of Irrigation and Drainage Engineering* 138(6): 548-552, (2011).
- [4] Emiroglu ME, Kaya N and Agaccioğlu H. Discharge capacity of labyrinth side weir located on a straight canal. *Journal of Irrigation and Drainage Engineering*, 136(1): 37-46, (2010).
- [5] Emiroglu ME, Kaya N and Agaccioğlu H. Closure to “Discharge Capacity of Labyrinth Side Weir Located on a Straight Canal” by M. E. Emiroglu, Nihat Kaya, and Hayrullah Agaccioğlu. *Journal of Irrigation and Drainage Engineering*, 137(11): 745-746, (2011).
- [6] De Marchi G. Essay on the performance of lateral weirs. *L'Energia Elettrica*, Milan, 11(11): 849-860 (in Italian), (1934).
- [7] Bonakdari H, Zaji AH, Shamshirband S, Hashim R and Petkovic D. Sensitivity analysis of the discharge coefficient of a modified triangular side weir by adaptive neuro-fuzzy methodology. *Measurement* 73: 74-81, (2015). 156(2): 185-191, (2003).
- [8] Seyedian SM, Ghazizadeh MJ and Tareghian R. Determining side weir discharge coefficient using Anfis. *Proceedings of the Institution of Civil Engineers - Water Management*, 167(4): 230-237, (2014).
- [9] Aydin M.C, “New Approach for Estimation of Rectangular Side Weirs Discharge in Subcritical Flow”, *Journal of Irrigation and Drainage Engineering (ASCE)*, 2016, 142(5): 10.1061/(ASCE)IR.1943-4774.0001014, 04016012.
- [10] Aydin M.C. Kayisli K., “Prediction of Discharge Capacity over Two-Cycle Labyrinth Side Weir Using ANFIS”, *Journal of Irrigation and Drainage Engineering*, 2016, 142(5): 10.1061/(ASCE)IR.1943-4774.0001006, 06016001
- [11] Aydin M.C., "CFD simulation of free-surface flow over triangular labyrinth side weir", *Advances in Engineering Software*, 45; 159-166 pp., 2012, DOI: 10.1016/j.advensoft.2011.09.006
- [12] Schmidt M. Zur Frage des abflusses uber streichwehre. *Techaniv Berlin-Charlottenbury, Mitteilung*, NY41, pp. 1-68 (in German), (1954).
- [13] Cheong HF Discharge coefficient of lateral diversion from trapezoidal canal. *Journal of Irrigation and Drainage Engineering* 117(4): 461-475, (1991).
- [14] Borghei SM, Nekooie MA, Sadeghian H and Ghazizadeh MRJ. Triangular labyrinth side weirs with one and two cycles. *Proceedings of the Institution of Civil Engineers - Water and Maritime Engineering* 166(1): 27-42, (2011).
- [15] Paris E, Solari L, Bechi G. Applicability of the De Marchi hypothesis for side weir flow in the case of movable beds, *Journal of Hydraulic Engineering* 138(7): 653-656, (2012).

- [16] Michelazzo G, Minatti L, Paris E and Solari L. Side weir flow on a movable bed. *Journal of Hydraulic Engineering* ISSN 0733-9429, 04016007, (2016).
- [17] Ozbek T. Open canal hydraulics and hydraulic structures. Technical Press, Turkey, Chapter 7, pp. 283-305 (in Turkish), (2009).
- [18] Emiroglu ME and Kaya N. Discharge coefficient for trapezoidal labyrinth side weir in subcritical flow. *Water Resources Management* 25(3): 1037-1058, (2011).
- [19] Kirkgoz MS, Ardicioglu M. Velocity profiles of developing and developed open canal flow. *Journal of Hydraulic Engineering* 123(12): 1099-1105, (1997).
- [20] El-Khashab AMM. Hydraulic of flow over side weirs. (Ph.D. Thesis), Presented to the University of Southampton, England, (1975).
- [21] El-Khashab AMM and Smith KVH. Experimental investigation of flow over side weirs. *Journal of Hydraulic Division* 102(Hy9): 1255-1268, (1976).
- [22] Subramanya K and Awasthy SC. Spatially varied flow over side-weirs. *Journal of the Hydraulics Division* 98(1): 1-10, (1972).
- [23] Hager WH. Lateral outflow over side weirs. *Journal of Irrigation and Drainage Engineering* 113(4): 491-504, (1987).
- [24] Borghei SM, Jalili MR and Ghodsian M. Discharge coefficient for sharp-crested side weir in subcritical flow. *Journal of Hydraulic Engineering* 125(10), 1051-1056, (1999).
- [25] Borghei SM, Vatannia Z, Ghodsian M and Jalili M R. Oblique rectangular sharp-crested weir. *Proceedings of the Institution of Civil Engineers - Water and Maritime Engineering*
- [26] Agaccioglu H, Emiroglu ME and Kaya N. Discharge coefficient of side weirs in curved canals. *Proceedings of the Institution of Civil Engineers - Water Management* 165(6): 339-352, (2012).
- [27] Borghei SM and Parvaneh A. Discharge characteristics of a modified oblique side weir in subcritical flow. *Flow Measurement and Instrumentation* 22: 370-376, (2011).
- [28] Ura M, Kita Y, Akiyama J, Moriyama H and Kumar JA. Discharge coefficient of oblique side-weirs. *Journal of Hydrosience and Hydraulic Engineering* 19(1): 85-96, (2001).
- [29] Emin Emiroglu, M., Cihan Aydin, M., and Kaya, N. Discharge characteristics of a trapezoidal labyrinth side weir with one and two cycles in subcritical flow. *Journal of Irrigation and Drainage Engineering*, 140(5), 04014007, (2014).